

Analysis of Stub Loaded Circular Microstrip Antennas

Amit A. Deshmukh¹, Ankit G.¹, Harsh C.¹,

Rahil S.¹ and Sneha S.¹

1. DJSCOE, Vile – Parle (W), Mumbai – 400 056

E-mail: amitdeshmukh76@rediffmail.com

K. P. Ray²

2. SAMEER, I.I.T. Campus, Powai – 400 076, Mumbai

E-mail: kpray@rediffmail.com

Abstract— Dual band circular microstrip antenna is realized by placing an open circuit stub on the edges of the patch. The stub is said to introduce capacitive and inductive impedance around the resonance frequency of the patch and realizes dual frequency response. The multi-band circular microstrip antenna is realized by placing two open circuit stubs on the opposite edges of the circular patch. In this paper, an open circuit stub loaded dual and triple band circular microstrip antennas are discussed. The analysis to study the dual and multi-band response of stub loaded circular microstrip antenna is presented. The resonance curve plots, surface current distributions and the radiation pattern plots over wide frequency range for different stub lengths were studied. It was observed that the placement of the stub modifies the fundamental and higher order mode resonance frequencies of the circular patch and realizes dual and multiple frequencies. The stub modifies the directions of surface currents on the patch and thereby gives broadside radiation pattern at first two frequencies.

Keywords- Circular microstrip antenna, dual band microstrip antenna, open circuit stub, higher order modes

I. INTRODUCTION

The dual band microstrip antenna (MSA) is realized by placing an open circuit stub of nearly quarter wave in length or short circuit stub of nearly half wave in length on the edges of the patch [1, 2]. It is a general understanding in these stub loaded MSAs that the stub offers capacitive impedance for the frequencies below the resonance frequencies of the patch and inductive impedance for the frequencies above the resonance frequencies of the patch and yields dual band response. Based on quarter and half wavelength approximation, the design equations for stub dimensions for desired dual frequencies are reported [3]. However these reported design equations are complex. Also the quarter wave or half wave approximation of length against the frequency does not give closer results for different stub lengths. In this paper, an analysis of open circuit single and dual stub loaded circular MSA (CMSA) for different stub length and width over a wide frequency range is presented. The simulated resonance curve plots, surface current distributions and radiation pattern plots for equivalent CMSA and single and dual stub loaded CMSA, were studied. In single stub loaded CMSA, the stub modifies the resonance frequencies of fundamental TM_{11} and higher order TM_{21} modes of the circular patch and

yields dual band characteristics. The stub modifies the directions of surface currents on the patch and gives similar radiation pattern characteristics (broadside) at the dual frequencies. The placement of single stub also modifies the higher order mode (TM_{31} and TM_{02}) resonance frequencies. Further the placement of second stub on the opposite edge of the patch modifies the TM_{11} , TM_{21} , TM_{31} and TM_{02} mode resonance frequencies of the stub loaded CMSA and yields multi-band characteristics. The radiation pattern at modified TM_{31} and TM_{02} modes is conical with higher cross-polarization levels. Thus the stubs do not introduce any mode but modifies the resonance frequencies of higher order modes of the circular patch and yields multi-band characteristics. The analysis is carried out using the IE3D software on glass epoxy substrate ($\epsilon_r = 4.3$, $\tan \delta = 0.02$ and $h = 0.16$ cm) [4].

II. DUAL BAND STUB LOADED CMSAS

The dual band stub loaded CMSA is shown in Fig. 1(a). The stub of length 'l' and width 'w' is placed on the edge of the circular patch. For the dimensions shown in Fig. 1(a), the simulated dual frequencies and BW's are 780, 980 MHz and 11, 12 MHz, respectively as shown in Fig. 1(b). The measured dual frequencies and BW's are 794, 971 MHz and 12, 10 MHz, respectively. The radiation pattern at dual frequencies is in the broadside direction with cross-polarization levels less than 15 dB as compared to that of the co-polar levels. The multi-band frequency response is realized by placing another stub on the opposite edge of single stub loaded CMSA as shown in Fig. 1(c). A triple frequency response is obtained as for given feed point location an impedance matching at three frequencies is realized as shown in Fig. 1(d). The simulated triple frequencies and BW's are 711, 1044 and 1466 MHz and 9, 11, 20 MHz, respectively. The measured triple frequencies and BW's are 702, 1032 and 1478 MHz and 10, 12, 23 MHz, respectively. The fabricated prototype of dual stub loaded CMSA is shown in Fig. 1(e). The radiation pattern at the first two frequencies is in the broadside direction whereas the pattern at third frequency is conical. While designing single and dual stub loaded CMSA at desired frequencies the quarter wavelength approximation of stub length does not give closer results. Therefore an analysis of stub loaded CMSA over a wide frequency range is carried

out. First the equivalent CMSA is analyzed as discussed in the following section.

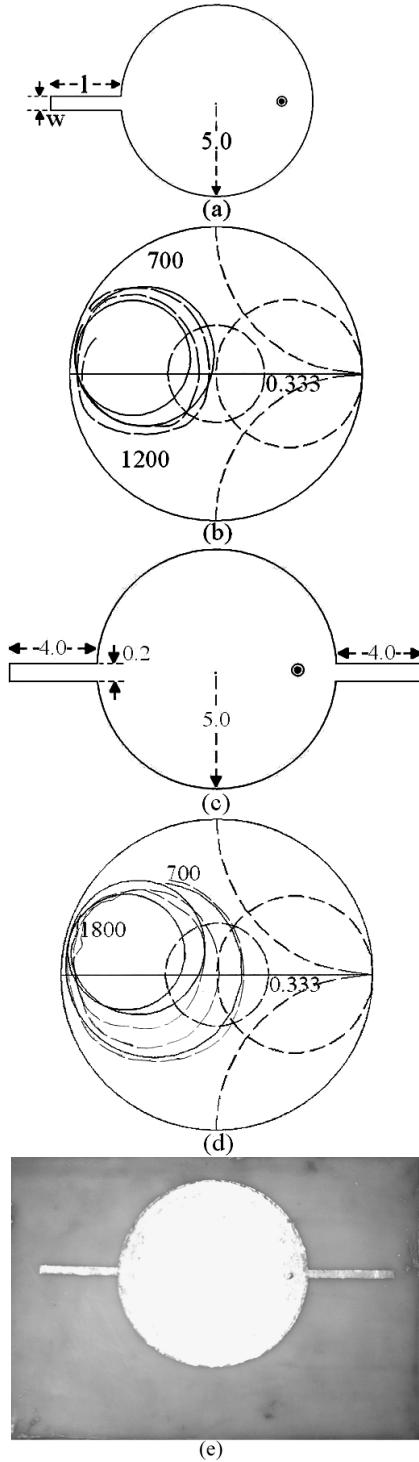


Fig. 1 (a) Single stub loaded CMSA and its input impedance plots, (—) simulated, (---) measured, (c) dual stub loaded CMSA and its (d) input impedance plots, (—) simulated, (---) measured, and (e) fabricated prototype of dual stub loaded CMSA

III. ANALYSIS OF STUB LOADED CMSA

The resonance frequency of CMSA is calculated by using equation (1) [1]. For radius of $r = 5.0$ cm, the various resonance frequencies are, $f_{TM11} = 899$ MHz, $f_{TM21} = 1443$ MHz, $f_{TM02} = 1756$ MHz, $f_{TM31} = 1984$ MHz. The CMSA was simulated using IE3D software and its resonance curve plot is shown in Fig. 2(a). The simulated resonance frequencies are $f_{TM11} = 868$ MHz, $f_{TM21} = 1407$ MHz, $f_{TM02} = 1729$ MHz, $f_{TM31} = 1944$ MHz. The surface current distributions at various modes are shown in Fig. 2(b – d).

$$f_r = \frac{K_{mn}c}{2r_e\pi\sqrt{\epsilon_r}} \quad (1)$$

where, f_r = resonance frequency of TM_{mn} mode,
 c = velocity of light = 3×10^8 (m/s)

K_{mn} is the m^{th} zero of the derivative of the Bessel function of n^{th} order, which is = 1.84118 (TM_{11}), 3.05424 (TM_{21}), 3.83171 (TM_{02}), 4.20119 (TM_{31}), 5.317 (TM_{41}), 5.3314 (TM_{12}), m and n = mode index

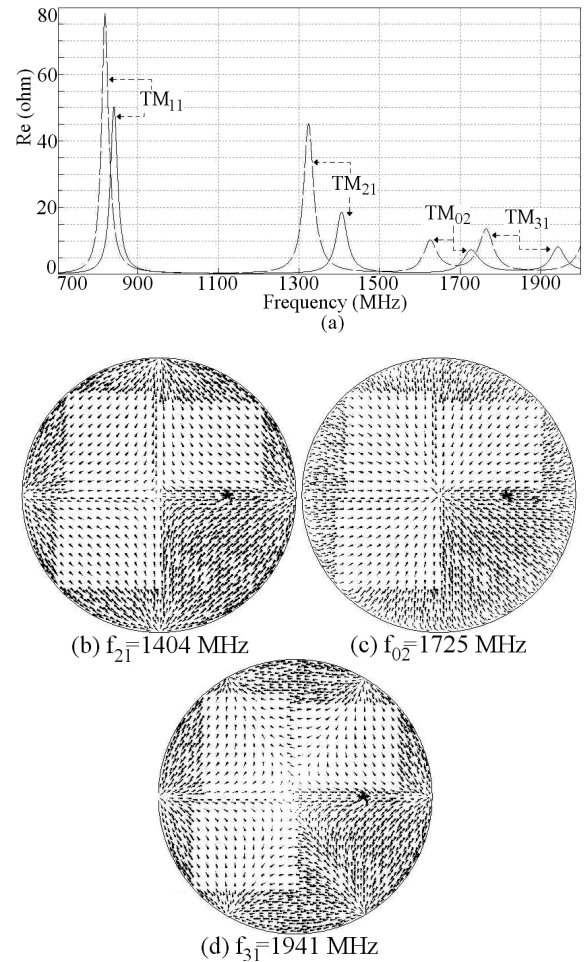


Fig. 2 (a) Resonance curve plots for (—) CMSA and (---) stub loaded CMSA and (b – d) surface current distributions for CMSA

At TM_{21} mode, surface currents shows two half wavelength variations along half of the patch perimeter and one half wavelength variation along the patch diameter. At TM_{02} mode the currents show two half wavelength variations along the patch diameter whereas field is constant along the patch perimeter. At TM_{31} mode, currents shows three half wavelength variations along half of the perimeter of the patch and one half wavelength variation along the patch diameter. The radiation pattern at TM_{11} mode is in the broadside direction whereas the pattern at TM_{21} , TM_{31} and TM_{02} modes is conical. Further an open circuit stub is placed on the edge of the patch as shown in Fig. 1(a). The stub length is varied from 1 to 6 cm in steps of 0.5 cm and for each of the length resonance curve plots, surface current distributions and simulated radiation pattern at each of the modes were studied. For $l = 2$ cm and $w = 0.4$ cm, the resonance curve plot is shown in Fig. 2(a). The surface current distributions at modified TM_{11} and TM_{21} modes are shown in Fig. 3(a, b). As seen from the resonance curve plots and surface current distributions that the stub modifies the resonance frequency of TM_{21} mode and along with the TM_{11} mode yields dual band characteristics. With increasing stub length the surface currents distributions at TM_{21} mode are modified such that they are similar to the current distributions at TM_{11} mode. Hence radiation pattern at modified TM_{21} mode is in the broadside direction as shown in Fig. 4. The placement of single stub has also modified the frequencies of TM_{31} , TM_{41} and TM_{02} modes. The surface current distributions at modified TM_{31} and TM_{02} modes are shown in Fig. 3(c, d). The formulation of resonant length at modified TM_{11} and TM_{21} mode in terms of stub dimension is obtained by using equations (2) – (5). The ‘A’ is the weighting function whose value depends upon variation in TM_{mn} mode frequency with respect to stub length.

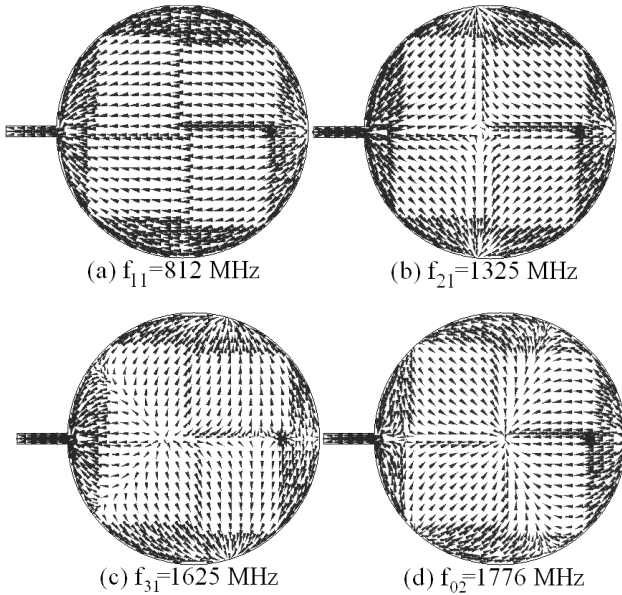


Fig. 3 (a – d) Surface current distributions for stub loaded CMSA

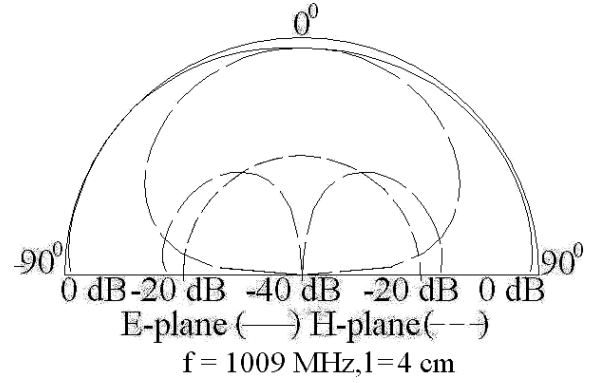


Fig. 4 Radiation pattern at modified TM_{21} mode for stub loaded CMSA

At f_1 ,

$$r_e = r + \left(\frac{w}{2}\right) + (0.285Al) \quad (2)$$

$$f_r = \frac{1.84118c}{2r_e \pi \sqrt{\epsilon_{re}}} \quad (3)$$

At f_2 ,

$$r_e = r + \left(\frac{w}{2}\right) + (0.721Al) \quad (4)$$

$$f_r = \frac{3.5424c}{2r_e \pi \sqrt{\epsilon_{re}}} \quad (5)$$

For $w = 0.2$ cm, frequencies calculated using above formulation at modified TM_{11} and TM_{21} mode, closely agrees with simulated frequencies with an error of less than 5%, as shown in Fig. 5 and 6, respectively.

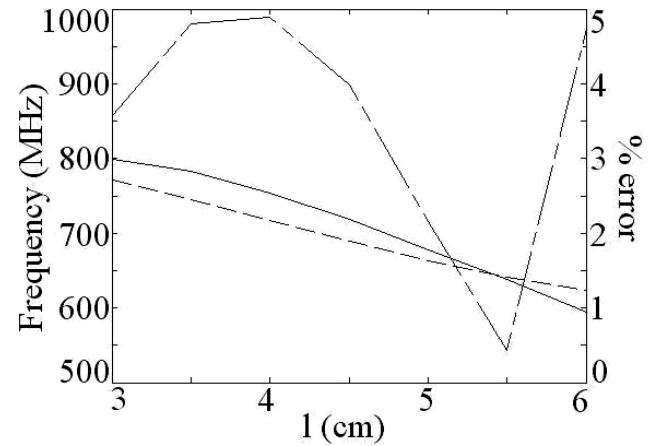


Fig. 5 Frequency and error plots for stub loaded CMSA at modified TM_{11} mode, (—) simulated, (---) calculated, (.....) % error

Further to realize multi-band CMSA, another open circuit stub is placed on the other edge of single stub loaded CMSA as shown in Fig. 1(c). The resonance curve plot for second stub of length 2 and 3 cm with resonance curve plots of CMSA with single stub of length 4 cm are shown in Fig. 7(a, b).

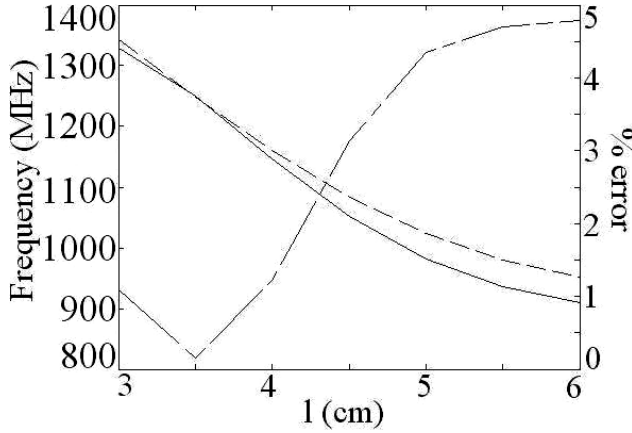


Fig. 6 Frequency and error plots for stub loaded CMSA at modified TM_{21} mode, (—) simulated, (---) calculated, (.....) % error

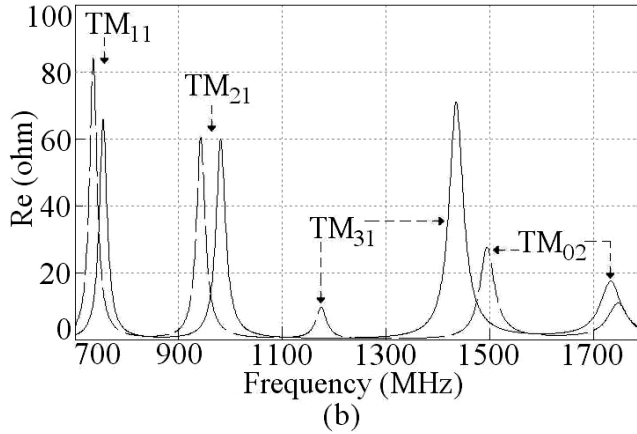
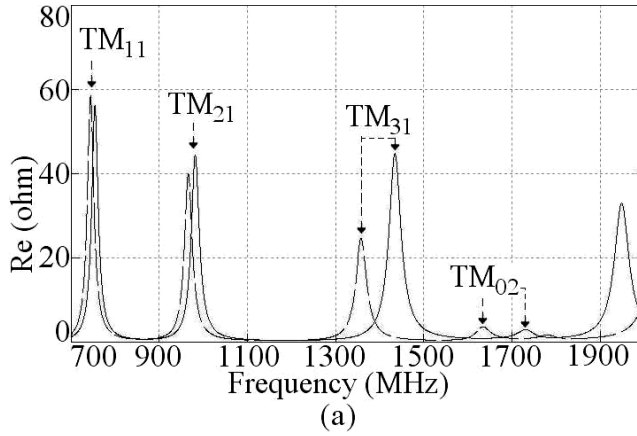


Fig. 7 Resonance curve plots for dual stub loaded CMSA for stub length of (a) 2 cm and (b) 3 cm, (—) CMSA, (---) CMSA with stub

With an increase in second stub length, the resonance frequencies of all the modes (i.e. TM_{11} , TM_{21} , TM_{31} and TM_{02}) decrease. The surface current distribution at modified TM_{31} and TM_{02} modes for second stub length of 2.0 cm are shown in Fig. 8(a, b). The current distribution at these modes is perturbed due to the presence of dual stubs.

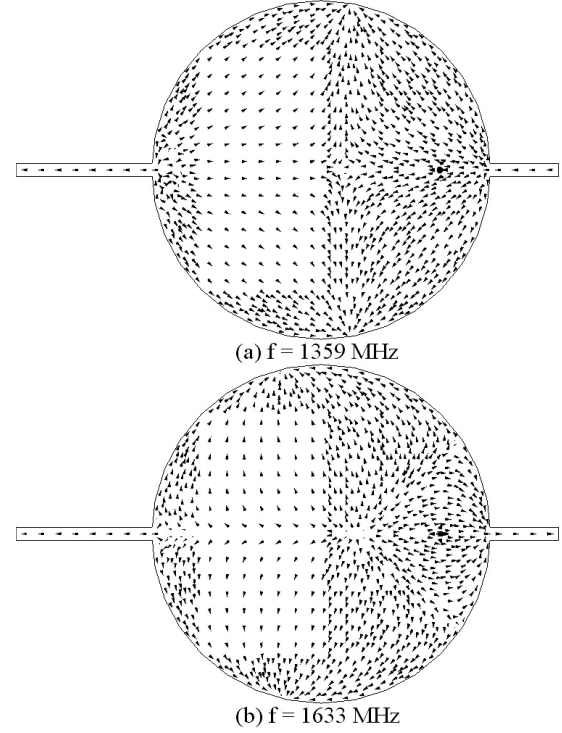


Fig. 8 Surface current distribution for dual stub loaded CMSA at modified (a) TM_{31} and (b) TM_{02} modes

Further increase in the stub length, decreases the resonance frequencies of these modes and realizes multi-band frequency response. Since the vertical components of the surface currents are present modified TM_{31} and TM_{02} modes in the circular patch, the radiation pattern is conical with higher cross polarization levels.

IV. CONCLUSIONS

The analysis of single and dual stub loaded CMSAs are presented. In single stub loaded CMSA, an open circuit stub modifies the resonance frequencies of fundamental TM_{11} and higher order TM_{21} modes and realizes dual frequency response. At TM_{21} mode the directions of surface currents are modified with increasing stub length and thereby yields broadside radiation pattern. The placement of stub also modifies the resonance frequencies of TM_{31} and TM_{02} modes. Further when the second stub is placed on the other edge, it modifies the frequencies of TM_{31} and TM_{02} modes and along with modified TM_{11} and TM_{21} modes realizes multi-band frequency response.

REFERENCES

- [1] G. Kumar and K. P. Ray, *Broadband Microstrip Antennas*, Artech House, USA, 2003
- [2] K. L. Wong, *Compact and Broadband Microstrip Antennas*, John Wiley & sons, Inc., New York, USA, 2002
- [3] A. E. Daniel, *Tunable Dual Band Rectangular Microstrip Antennas And Their Arrays*, Ph.D. Thesis, I. I. T. Bombay, 2006.
- [4] IE3D 12.1, Zeland Software, Freemont, USA